Available online at www.sciencedirect.com

ScienceDirect

Journal of the Franklin Institute xxx (xxxx) xxx

www.elsevier.com/locate/jfranklin

Tuning procedure for event-based PI controllers under regular quantization with hysteresis

Oscar Miguel-Escrig*, Julio-Ariel Romero-Pérez

Department of System Engineering and Design, Universitat Jaume I. Campus del Riu Sec Avda, Vicent Sos Baynat s/n 12071, Castelló de la Plana, Spain

Received 14 September 2020; received in revised form 2 February 2021; accepted 2 April 2021
Available online xxx

Abstract

In this paper a tuning procedure is proposed for event based PI controllers with Regular Quantization with Hysteresis (RQH) sampling law. The RQH is a generalization of Symmetric Send on Delta (SSOD) strategy which decreases the robustness requirements to avoid limit cycle oscillations and reduce the number of events needed for control, improving the overall performance of PI controllers in networked control systems. The tuning procedure takes into account not only classical robustness margins but also takes advantage of some specific robustness measures to avoid limit cycle oscillations induced by the sampler. As the robustness analysis depends on the Describing Function (DF) method, a study evaluating the effect of high order harmonics is provided, showing the validity of the tuning procedure. Some examples are included in which the usefulness of the tuning procedure is shown.

1. Introduction

Event based control (EBC) of continuous system is getting more and more attention recently [1]. This is due to some of the advantages that EBC offers, such as providing a better management of the data flow through the digital networks on distributed control systems, reducing the data drop out in the form of package losses and decreasing the delays caused by the communication. These benefits are a direct consequence of the EBC data transmission policy, which consists in sending data only when significant changes are detected on the state

* Corresponding author.
E-mail addresses: omiguel@uji.es (O. Miguel-Escrig), romeroj@uji.es (J.-A. Romero-Pérez).

https://doi.org/10.1016/j.jfranklin.2021.04.004
0016-0032/

of the system and not periodically as in most of classical control loops. In networked control systems the EBC approach may be considered among the most promising control approaches, in deed, in [2] its importance in modern factory automation has been recently highlighted.

In [3] a summarized but extensive study about the main contributions on EBC in the last two decades is presented. The results in that paper revels scarce of investigation on event based PID respect to other control approaches such as Model-based, Predictive or State-feedback control. PID, however, is used in most of the industrial control applications. Due to the high sensitivity of the derivative action to the measurement noise, the PI control is the dominant form of the PID in use today, [4]. This dominance in the industrial environment over other advanced control strategies such as MPC, was reflected in a survey conducted among the industrial committee members of the International Federation of Automatic Control published in [5]. The versatility of PID algorithms also allows them to remain important in the modern context of Industry 4.0 as it was highlighted in [6], where the necessity of introducing new features to the PID algorithms in order to adapt them to the high connectivity between devices through wired and wireless communication networks that this paradigm offers was also pointed out. The adaptation of PID to the paradigm of event based control can contribute to its use in this new application scenarios.

In EBC systems, the event generation policy is of paramount importance because it is in charge of generating and sending the events that regulate the execution of the controller algorithm, which, as shown in [7], determines the performance and behavior of sampled control systems. The most used event generation techniques, mainly because of their simplicity of implementation, are the ones based on the signal quantification, like the send-on-delta (SOD) sampling technique, which is based on sending new events when the sampled signal changes in more than a threshold δ. The effectiveness of this strategy has been tested in terms of control performance and communication reduction, [8,9].

To the knowledge of the authors, the use of SOD in PID control loops was introduced by rzn [10] to reduce the use of CPU in embedded control systems without significantly degrading the system performance. To do that, the sensor is sampled periodically but the control algorithm is executed only if the error signal crosses preset thresholds. Some further works were focused on solving the problems raised by rzn, mainly related with the calculation of the integral of error when the time between samples increases. It should be noted in particular the works of Durand [11,12] and Vasyutynskyy [13,14]. Recent works have extended the rzn proposal to fractional order systems. Concretely, the implementation issues of the discrete event-based fractional order controllers have been addressed for two different control algorithms: FO-IMC [15] and FO-PID [16–18]. Because the aim of these papers is to reduce the computation effort of the control algorithms, their main contribution is the development of control routines computationally more efficient. However, no tuning procedures have been developed for these algorithms taking into account the effect of the SOD sampler, and the use of tuning methods for continuous controllers is suggested instead.

With similar principles than in SOD sampling, in [19] a sampling strategy known as symmetric-send-on-delta (SSOD) was presented, being the main characteristic traits the inclusion of a hysteresis with the same magnitude than the quantification threshold δ and having fixed switching levels. Several works have been published with regard to SSOD sampling in loops with a PI controller, concerning tuning procedures, identification and application cases. In [20], a tuning procedure for PI controllers in SSOD sampling was presented taking into account first order plus time delay (FOPTD) models, and some rules were designed by minimizing the 1% settling time of the closed loop response. SSOD sampler has also been

used for identification, for instance, in [21] a system identification procedure was proposed. In [22], event-based controllers with a SSOD sampling strategy were applied to the inside air temperature control of the greenhouse production process.

In [23,24], some tuning methods for PI controllers with SSOD sampler have been developed. Additionally, in [25] a unified design of a SSOD based PID and Smith predictor for self-regulating and integral processes was investigated. The approach followed in these publications was based on some robustness margins to avoid limit cycles that were obtained by applying the describing function (DF) technique, whose used allowed to introduce the classical concepts of phase and gain margins in the design of this kind of EBC. The DF is a well-known analysis tool for Wiener-Hammerstein nonlinear systems introduced in the 30s, and posteriorly presented in [26]. Several variants based on this technique were presented, e.g. the dual input DF [27], the sampled or discrete DF [28] and the fractional order DF [29]. A lot of literature can be found about this method, for example in [30,31].

Another sampling strategy based on the signal quantization is the Regular Quantification (RQ) sampling strategy, which is an alternative to SSOD event generation, and consist in sending new data whenever the value of the sampled signal is a multiple of the quantization threshold δ. A comparative study between SSOD and RQ strategies was presented in [32]. Due to the lack of hysteresis in the RQ sampler, the measurement noise can produce bursts of events, and thus, bursts of data to transmit, which is the main disadvantage of RQ with respect to SSOD. Nevertheless, the inclusion of the hysteresis, as in the case of SSOD, forces the controller to fulfill higher robustness requirements to avoid limit cycle oscillations.

Taking these effects of the hysteresis into account, in [33] a new sampling strategy called Regular Quantization with Hysteresis (RQH) was presented. This sampling strategy consists of a quantification with fixed thresholds and with variable hysteresis, which can be chosen freely, and depending on these parameters choice the intermediate cases between the RQ and SSOD appear. In that work the event generation for the same process reactivity was characterized and the robustness against limit cycle oscillations studied, introducing new gain and phase robustness margins to the presence of this kind of oscillations.

Using these new margins, it has been proved that in general the tuning methods for continuous PI do not provide good enough results when applied to PI controllers with RQH sampling since either the limit cycles are not avoided or, conversely, extremely robust controllers are obtained which is an indicator that faster behavior can be achieved. This fact evidenced the necessity for developing new tuning algorithms for this kind of control systems taking into account the effects of the RQH sampler in order to improve the trade-off between robustness and speed of response.

In this paper, a tuning procedure for PI controllers within a loop in which the error signal is sampled according to the RQH principles is proposed. The procedure takes into account classical robustness measures such as gain and phase margin, as well as it includes specific robustness measures, also in terms of gain and phase, to the oscillations induced by the sampler in the loop, which were presented in [33]. The tuning procedure and the obtained margins are tested in simulation for several processes which prove the tuning procedure applicability. Additionally, the validation of any controller placed within a structure with an RQH sampling is studied by taking into account additional harmonics which have an effect on the robustness measures.

The paper is organized as follows. Section 2 presents the main characteristics and advantages of the RQH sampling strategy and highlights the necessity of a specific tuning method. Section 3 proposes a tuning procedure for the controller placed in a loop with a RQH

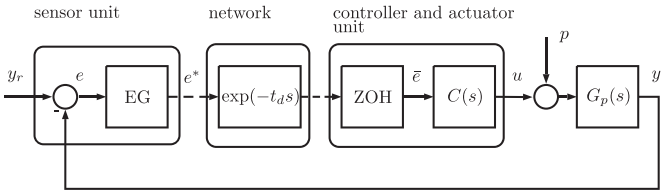

Fig. 1. Control loop scheme for event-based PID controllers proposed in [19].

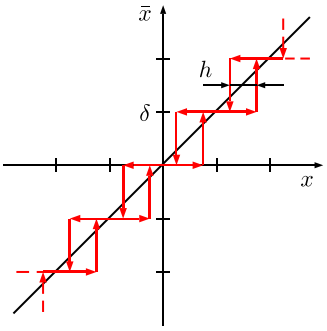

Fig. 2. Relationship between input x and output $\bar{x}$ for the RQH sampling strategy.

sampler. This tuning procedure takes into account both classical and specific to the non-linearity robustness margins. Section 4 studies the validation of controllers placed in this kind of loops by considering the effect of high order harmonics. Finally, the conclusions about this work are drawn.

2. Problem statement

The typical networked control system in which event generators such as the RQH are placed is presented in Fig. 1. In this figure, the controller and process are denoted by the blocks $C(s)$ and $G_p(s)$ respectively, the applied sampler, or event generator, is represented by the EG block, the ZOH block is a zero-order hold and the network's delay is modeled by $\exp(-t_d s)$. The reference signal to track is denoted by y_r, the controlled output by y and the disturbance signal by p. The controller is assumed to be placed close to the actuator. The measured signal e^* of the error e is sent by the event generator through the communication network and the ZOH block keeps in $\bar{e}$ the last value sent until new data arrive. This control scheme was first proposed in [19] considering that the EG block was a SSOD and the controller a PI. Instead of the SSOD, in this work the RQH sampling will be used in the EG block.

The RQH sampler is defined essentially by two parameters, the quantization level $\delta > 0$ and the hysteresis h that can be freely selected as long as $0 \leq h \leq \delta$, being the ratio h/δ the characteristic parameter that define most of the sampler properties. The relation between an input x and its output $\bar{x}$ of the RQH sampler is presented in Fig. 2. In this figure the RQ or SSOD samplers input/output relationship can be obtained by fixing $h = 0$ or $h = \delta$ respectively, being the RQH a more general strategy that embraces both, which consequently, presents characteristics that are a trade-off between RQ and SSOD. Namely, immunity to generate events caused by noise in the signal, low event generation for the same reactivity to

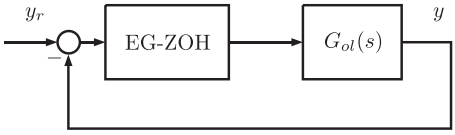

Fig. 3. Block scheme equivalent to the one presented in Fig. 1.

changes and lesser robustness requirements for the controller to avoid limit cycle oscillations than the SSOD sampler.

To select the proper parameters for the RQH sampler a simple procedure was presented in [33]. Firstly, the hysteresis h is selected slightly greater than the peak-to-peak amplitude of the measure noise to prevent it from generating events. Secondly, the parameter δ is selected to assure a certain reactivity to significant changes on the system, which are defined by the steady-state error e_{ss}. The RQH sampling, as well as SSOD and RQ strategies, introduces a steady-state error on the controlled output y, this is due to the existence of a dead band around $e = 0$ in which the sampler will send $\bar{e} = 0$ because the thresholds are not surpassed. The steady-state error in RQH samplers is defined by $e_{ss} = (\delta + h)/2$. If h has been previously chosen to avoid event generation due to the measurement noise, then δ can be obtained directly from this expression to fulfill the e_{ss} requirement. Additionally, the ratio h/δ of the RQH sampler has a big influence on the number of generated events, which increase proportionally with this ratio, thus, making the e_{ss} of the system to be the maximum admissible e_{ss}, by means of maximizing δ, decreases to the lowest possible the number of events generated for a given change in the signal to track.

Once the ratio h/δ is defined, the RQH can be characterized in terms of robustness using the Describing Function (DF) technique. To apply the DF technique, the block scheme presented in Fig. 1 can be rewritten as that in Fig. 3, in which the network delay, the control and process transfer functions are grouped in $G_{ol}(s) = G_p(s)C(s)e^{-t_d s}$, which is the open-loop transfer function of the system, and the rest in the block EG-ZOH. This last block presents the same behavior as the original blocks: it samples the signal and holds its value until new samples are taken. Therefore, the EG-ZOH results in a non-linearity which can be studied with the DF method.

The condition for the existence of limit cycle in the system presented in Fig. 3 is given by:

$$G_{ol}(j\omega) = -\frac{1}{\mathcal{N}}, \quad \forall\omega, \tag{1}$$

where $\mathcal{N}$ is the describing function of the non-linearity. Graphically, if it exists an intersection between the open-loop transfer function and the inverse negative of the DF, the system will present limit cycle oscillations. The DF for the RQH sampling strategy was presented in [33] and is given by the following equation:

$$\mathcal{N}(A,h) = \frac{2\delta}{A\pi}\left[\sum_{k=1}^{m}\sqrt{1-\left(\frac{\delta}{A}\left(k+\frac{h}{2\delta}-\frac{1}{2}\right)\right)^2} + \sum_{k=m+1}^{2m}\sqrt{1-\left(\frac{\delta}{A}\left(2m-k-\frac{h}{2\delta}+\frac{1}{2}\right)\right)^2}\right] - j\frac{2hm\delta}{A^2\pi}, \tag{2}$$

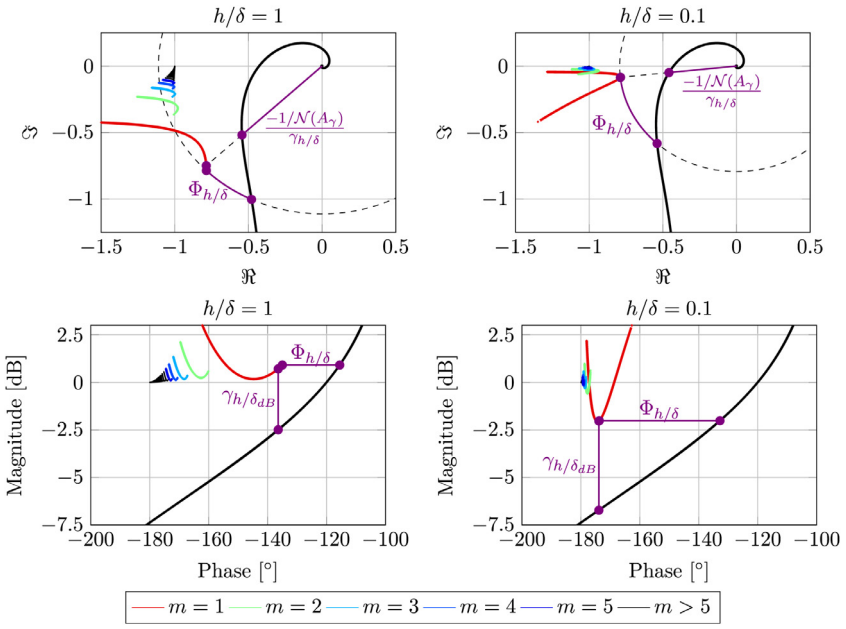

Fig. 4. Shapes of $-1/\mathcal{N}$ for RQH samplers with different values of h/δ in Nyquist and Nichols diagrams with the gain and phase margins to the non-linearity $\gamma_{h/\delta}$ and $\Phi_{h/\delta}$.

where A is the amplitude of the sinusoidal oscillation and $m = \left\lfloor \frac{A}{\delta} - \frac{h}{2\delta} + \frac{1}{2} \right\rfloor$ is the maximum number of levels crossed by the oscillation.

The traces of $-1/\mathcal{N}$ are composed of several branches, one for each value of m. As the ratio h/δ decreases, all the branches tend to fold and move towards the Real-axis, being a horizontal line when $h/\delta = 0$. In Fig. 4 the locus of $-1/\mathcal{N}$ for different values of h/δ is represented. The case where $h/\delta = 1$ represents the negative inverse of $\mathcal{N}$ for SSOD and several studies about its robustness have already been presented [32,34].

An important remark is that for PI controllers tuned with reasonable robustness margins the shape of G_{ol} is such that the non intersection with the branch corresponding to $m = 1$ guarantees to avoid intersections with branches for $m > 1$, and therefore, no intersection between G_{ol} and $-1/\mathcal{N}$ takes place, avoiding limit cycle oscillations.

Using the expression of the DF presented in Eq. (2), in [33], a study of the robustness against limit cycles of certain classical tuning methods was presented for a batch of processes. To that end, a gain $\gamma_{h/\delta}$ and phase $\Phi_{h/\delta}$ margins to the non-linearity were defined, revealing that some methods cannot be applied for certain ratios h/δ without presenting limit cycle oscillations, and other methods present an extremely robust behavior which can be an indicator that faster controllers can be tunned. These margins are presented in Fig. 4 in Nyquist and Nichols diagrams in violet.

In addition, unlike the classical phase and gain margins, an important consideration to be taken into account is that the robustness margins to the non-linearity $\gamma_{h/\delta}$ and $\Phi_{h/\delta}$ usually provide poor information about the closed loop performance. This is due to the fact that they are not measured with regard to a fixed point, instead, these measures depend on the non-linearity and on the open-loop transfer function shapes. In a similar way, assuring some

classical gain and phase margins, or using classical tuning rules, does not guarantee to avoid limit cycle oscillations induced by the sampling because it has not been taken into account in the original design. Thus, in this paper a tuning procedure which takes into account both classical margins and these new robustness margins to the non-linearity in the design procedure is developed.

3. Tuning procedure for RQH based PI

From the study presented in [33] and as it has been commented before, tuning methods for continuous PI are not entirely valid for designing controllers with RQH sampling strategy since $\Phi_{h/\delta}$ and $\gamma_{h/\delta}$ must be checked afterwards to ensure the avoidance of limit cycles. In this section, a tuning procedure for PI controllers will be introduced taking into account classical robustness measures and these new specific measures. The only restriction for the calculation of the new margins is the usage of the DF technique, which assumes the process to be filtering enough to neglect the high order harmonics effect. This means that the method can be used for a wide range of processes, having either sub-damped or over-damped response including time delays or non minimum phase.

Before applying the tuning procedure, the parameters h and δ that define the RQH describing function, and significantly affect the robustness measures, must be selected taking into account the admissible steady state error (e_{ss}) and the peak-to-peak amplitude of the measurement noise, as commented in Section 2. It is important to keep in mind that higher values of h/δ affect negatively the amount of events generated, which will be greater than the number of events generated with intermediate values of h/δ. Besides, the increase of this ratio affects in an inversely proportional way the controller's speed to attain the same margins $\Phi_{h/\delta}$ and $\gamma_{h/\delta}$.

Once the parameters δ and h have been selected, the shape of $-1/\mathcal{N}$ is defined, and the PI controller tuning procedure can be addressed. The goal of the tuning procedure proposed in this section is to obtain the controller that minimize the IAE (Integral of Absolute value of the Error) index of the disturbance response while fulfilling the requirements on gain and phase margins. This tuning problem can be expressed as follows:

$$\begin{aligned} \underset{K_p,T_i}{\text{minimize}} \quad & IE \\ \text{subject to} \quad & \gamma_{cg} \geq \gamma_{cg_r}, \Phi_{cp} \geq \Phi_{cp_r}, \\ & \gamma_{h/\delta} \geq \gamma_{h/\delta_r}, \Phi_{h/\delta} \geq \Phi_{h/\delta_r} \end{aligned} \tag{3}$$

where γ_{cg} and Φ_{cp} are the classical gain and phase margin, and the sub-index r refers to the required value of each parameter. It is well-known that for non-oscillatory responses the minimization of IAE and IE (Integral of the error) are equivalents. However, using the later is preferable because the IE is directly related with the controllers parameters trough the integral gain ($K_i = K_p/T_i$) which facilitates the solution of the optimization problem.

As commented before, the RQH sampling causes the apparition of a steady state error, and thus, that the integral of the error signal will tend to infinite. However, in Appendix A it has been proven that, with reasonable parameters, the integral of the sampled error signal is similar to the integral of the error signal in a continuous system, i.e. to the IE index.

Before describing the tuning procedure, it is important to note that the following conditions must be met in order to fulfill the margins restrictions in Eq. (3):

$$\text{Classical gain margin} \begin{cases} \left|G(j\omega_{cg})\right|\left|C(j\omega_{cg})\right| \leq 1/\gamma_{cg_r} & (4a) \\ \arg(G(j\omega_{cg})) + \arg(C(j\omega_{cg})) = -\pi & (4b) \end{cases}$$

$$\text{Classical phase margin} \begin{cases} \left|G_{ol}(j\omega_{cp})\right| = 1 & (5a) \\ \arg(G_{ol}(j\omega_{cp})) \leq -\pi - \Phi_{cp_r} & (5b) \end{cases}$$

$$h/\delta \text{ gain margin} \begin{cases} \left|G(j\omega_{\gamma})\right|\left|C(j\omega_{\gamma})\right| \leq \frac{1}{\gamma_{h/\delta_r}}\left|-\frac{1}{\mathcal{N}(A_{\gamma})}\right| & (6a) \\ \arg(G_{ol}(j\omega_{\gamma})) = \arg\left(-\frac{1}{\mathcal{N}(A_{\gamma})}\right) & (6b) \end{cases}$$

$$h/\delta \text{ phase margin} \begin{cases} |G_{ol}(j\omega_{\Phi})| = \left|-\frac{1}{\mathcal{N}(A_{\Phi})}\right| & (7a) \\ \arg(G_{ol}(j\omega_{\Phi})) \leq \arg\left(-\frac{1}{\mathcal{N}(A_{\Phi})}\right) - \Phi_{h/\delta_r} & (7b) \end{cases}$$

Where $G(s) = G_p(s)e^{-t_d s}$ is considered to take into account the process transfer function $G_p(s)$ and the communication delay modeled by $e^{-t_d s}$.

The precedent equations define a whole set of controllers whose margins will be at least the required values or greater. Our goal is to find the controller with maximum $K_i = K_p/T_i$ (minimum IE) in this set.

The tuning procedure consists of 3 steps:

1. Find the set of all the PI controllers that can be obtained for a given process.
2. Tune each controller obtained from step 1 according to the gain margin and detune those that do not fulfill the requirements on Φ_{cp}, $\gamma_{h/\delta}$ or/and $\Phi_{h/\delta}$.
3. Finally, choose among all the resulting controllers the one with minimum $IE = K_p/T_i$.

Next, these steps are described in detail.

Step 1 The tuning procedure starts by obtaining the range of possible values for ω_{cg}. Since for a PI controller $\arg(C(j\omega)) \in \left[-\frac{\pi}{2}, 0\right]$, the application of the Eq. (4b) implies that $\arg(G(j\omega_{cg})) \in \left[-\pi, -\frac{\pi}{2}\right]$. Thus, the range of ω_{cg} can be directly obtained from the phase response of $G(j\omega)$ as the values of ω within the boundaries defined by $\arg(G(j\omega)) = -\pi$ and $\arg(G(j\omega)) = -\frac{\pi}{2}$. For this range of ω_{cg} a regular griding is defined. Each item in the grid corresponds to a PI controller whose parameter will be calculated according to step 2.

Step 2 This step is applied to each item in the grid of ω_{cg} obtained in step 1. The value of T_i can be calculated using the equation of the PI phase

$$\arg(C(j\omega)) = \arctan(T_i\omega) - \frac{\pi}{2}, \tag{8}$$

that combined with Eq. (4b) result in,

$$T_i = \frac{1}{\omega_{cg}} \tan\left(-\arg(G(j\omega_{cg})) - \frac{\pi}{2}\right). \tag{9}$$

Once T_i has been obtained, the corresponding K_p can be calculated. K_p is firstly obtained to fulfill the restriction on γ_{cg}. For a PI controller, the modulus can be expressed as:

$$|C(j\omega)| = K_p \frac{\sqrt{1+(\omega T_i)^2}}{\omega T_i}. \tag{10}$$

Thus, from Eq. (4a) we obtain that:

$$K_p \leq \frac{\omega_{cg} T_i}{\gamma_{cg_r} \left|G(j\omega_{cg})\right| \sqrt{1+(\omega_{cg} T_i)^2}}. \tag{11}$$

As the objective is to optimize the IE index, the maximum gain K_p within all the possible values defined by Eq. (11) will be considered. That is:

$$K_p = \frac{\omega_{cg} T_i}{\gamma_{cg_r} \left|G(j\omega_{cg})\right| \sqrt{1+(\omega_{cg} T_i)^2}}. \tag{12}$$

At this point, the controller fulfills the classical gain margin restriction. To meet the rest of margin conditions, Eqs. (5a) to (7b) are checked and the controller is conveniently detuned if needed. This is based on the fact that reducing K_p implies a radial shrinking of $G_{ol}(j\omega)$ in the Nyquist diagram, or a downward displacement in the Nichols diagram. Consequently, the controller's detuning improves all the robustness margins.

In order to satisfy the classical phase margin requirement, Eq. (5) must be fulfilled. Considering in the construction of G_{ol} the values of K_p and T_i previously calculated, we obtain the current margin Φ_{cp}. If $\Phi_{cp} \geq \Phi_{cp_r}$, no modifications on K_p have to be done. However, if this requirement is not fulfilled, we obtain the frequency which will become the new ω_{cp} from Eq. (5b), forcing the equality

$$\arg(G_{ol}(j\omega_{cp})) = -\pi - \Phi_{cp_r} \tag{13}$$

A detuning factor k is then introduced to fulfill the Eq. (5a), whose value can be calculated as:

$$k = \frac{1}{\left|G_{ol}(j\omega_{cp})\right|} \tag{14}$$

Once k is obtained, the controller gain is recalculated as kK_p.

It is important to highlight that k shrinks the shape of $G_{ol}(j\omega)$ in the Nyquist diagram and consequently all the robustness margins are risen. Therefore, the conditions in (4) hold true and the design meets both gain and phase margins.

To fulfill the restrictions on $\gamma_{h/\delta}$ and $\Phi_{h/\delta}$ the procedure is similar to the one used with the classic margins. Firstly, the margin $\gamma_{h/\delta}$ is calculated and compared with γ_{h/δ_r}. If $\gamma_{h/\delta} < \gamma_{h/\delta_r}$, then k must be recalculated. From the definition of $\gamma_{h/\delta}$ it is worth noticing that for $kG_{ol}(j\omega)$ the factor k can be introduced as follows:

$$(\omega_\gamma, A_\gamma) = \arg\min_{(\omega,A)} \left(\frac{\left|-\frac{1}{\mathcal{N}(A)}\right|}{k|G_{ol}(j\omega)|} : \arg(G_{ol}(j\omega)) = \arg\left(-\frac{1}{\mathcal{N}(A)}\right) \right). \tag{15}$$

Since in the previous equation k does not affect the condition $\arg(G_{ol}(j\omega)) = \arg\left(-\frac{1}{\mathcal{N}(A)}\right)$ and $\frac{\left|-\frac{1}{\mathcal{N}(A)}\right|}{|G_{ol}(j\omega)|}$ is just scaled by $1/k$, then the frequency ω_γ and A_γ will

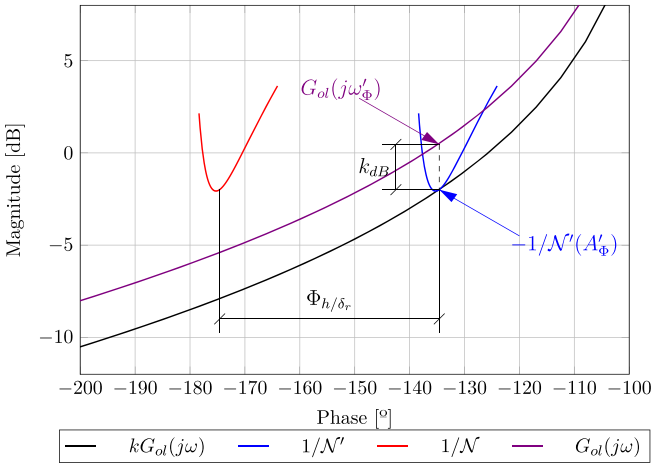

Fig. 5. Graphical interpretation of the detuning procedure to fulfill the Φ_{h/δ_r} margin.

remain invariable as k changes. Thus, the new value of k can be easily obtained from Eq. (6a):

$$k = \frac{1}{\gamma_{h/\delta_r}} \left| -\frac{1}{\mathcal{N}(A_\gamma)} \right| \frac{1}{|G_{ol}(j\omega_\gamma)|} \tag{16}$$

The last margin to check is the phase margin to the non-linearity, $\Phi_{h/\delta}$. If its value is greater than Φ_{h/δ_r}, then no modifications have to be done to the controller. On the other hand, if $\Phi_{h/\delta} < \Phi_{h/\delta_r}$ the parameter K_p must be recalculated. Let us consider the open-loop transfer function given by $kG_{ol}(j\omega)$, this parameter k can be introduced within the definition of the phase margin to the non-linearity as:

$$(\omega_\Phi, A_\Phi) = \arg\min_{(\omega,A)} \left(\arg(kG_{ol}(j\omega)) - \arg\left(-\frac{1}{\mathcal{N}(A)}\right) : \left| -\frac{1}{\mathcal{N}(A)} \right| = k|G_{ol}(j\omega)| \right). \tag{17}$$

In the previous expression the condition $\left| -\frac{1}{\mathcal{N}(A)} \right| = k|G_{ol}(j\omega)|$ depends on the value of k. This means that, unlike the cases of ω_γ and A_γ, ω_Φ and A_Φ depend on k. The new values of ω_Φ and A_Φ in which the phase margin will be measured once the detuning factor is introduced are calculated as:

$$(\omega'_\Phi, A'_\Phi) = \arg\max_{(\omega,A)} \left(|G_{ol}(j\omega)| - \left| -\frac{1}{\mathcal{N}'(A)} \right| \right). \tag{18}$$

where $-1/\mathcal{N}'(A) = -1/\mathcal{N}(A) \cdot 1\angle\Phi_{h/\delta_r}$. Then the detuning factor can be calculated as:

$$k = \left| -\frac{1}{\mathcal{N}'(A'_\Phi)} \right| \frac{1}{|G_{ol}(j\omega'_\Phi)|} \tag{19}$$

The graphical interpretation of this procedure is represented in Fig. 5. The detuning factor k is calculated to guarantee zero phase margin between kG_{ol} and $-1/\mathcal{N}'$, which

is an image of $-1/\mathcal{N}$ whose phase has been displaced Φ_{h/δ_r}. Consequently, the minimal distance in phase between kG_{ol} and $1/\mathcal{N}$, or in other words, the phase margin, is Φ_{h/δ_r}.

Step 3 Finally, as a result of the preceding steps a set of controllers defined by pairs (K_p, T_i) is obtained. Among them, the one that minimizes the IE index is selected as the resulting controller, which, for PI controllers, is the one that maximizes the ratio K_p/T_i.

Remark 1. In some applications, an important issue to consider is the wear of the actuator, which could be reduced by limiting the control action bumps produced by the steps of magnitude δ introduced by the RQH sampler in the input of the controller. For a PI controller these bumps have amplitude $\delta_u = K_p\delta$. Using this equation it is possible to obtain the maximum K_p for given values of δ and admissible control action bumps $\delta_{u_{\max}}$: $K_{p_{\max}} = \delta_{u_{\max}}/\delta$. Then, all the proportional gains obtained in step 2 that surpass $K_{p_{\max}}$ must be limited to this value.

Remark 2. Networked systems often contain communications delays, modeled in Fig. 1 by the $exp(-t_d s)$ block. In the presented procedure this delay must be added to the process transfer function delay if it exists. Introducing delay in the loop reduces all the studied robustness margins, therefore, not considering it in the process transfer function ($G(s) = G_p(s)exp(-t_d s)$) could lead to a potential loss of robustness, causing the apparition of limit cycle oscillations or even instability. Thus, if this communication delay is known it has to be considered into the process transfer function to perform the tuning procedure.

Remark 3. This tuning method can be applied to other type of controllers as long as the separation between linear and non-linear part presented in Fig. 3 is kept. For example, for a PID controller the Eqs. (8) and (10) result in:

$$\arg(C(j\omega)) = \arctan\left(\frac{\omega T_i(NT_i/T_d + 1)}{NT_i/T_d - (\omega T_i)^2(1+N)}\right) - \arctan\left(\frac{\omega T_i}{NT_i/T_d}\right) - \frac{\pi}{2}, \tag{20}$$

$$|C(j\omega)| = K_p \frac{\sqrt{(\omega T_i(NT_i/T_d + 1))^2 + (NT_i/T_d - (\omega T_i)^2(1+N))^2}}{\omega T_i\sqrt{(\omega T_i)^2 + (NT_i/T_d)^2}} \tag{21}$$

respectively, and it has to be taken into account that the range for the controller's phase is $\left[-\frac{\pi}{2}, \frac{\pi}{2}\right]$, changing the expressions derived from Eqs. (4)–(7). In this case, as more parameters are introduced (T_d and N), additional requirements could be considered for the design. A very important issue to be taken into account when considering other controllers is that the filtering properties of G_{ol} must be enough to kept the DF technique valid for predicting the limit cycle oscillation. This study can be done according to the procedure presented in Section 4 to validate the design of the PI.

The procedure is summarized in a flowchart which can be found in Fig. B.17 in Annex Appendix B. Note that once the pair (K_p, T_i) to fulfill the requirements on γ_{cg} is obtained, the remaining robustness measurements are tested and the controller gain is corrected if needed. Each margin is calculated, and if they are lower than the requirement, K_p is reduced according to a detuning factor k that is calculated with the pertinent equations.

In order to show the validity of the proposed tuning methodology let us introduce the following example.

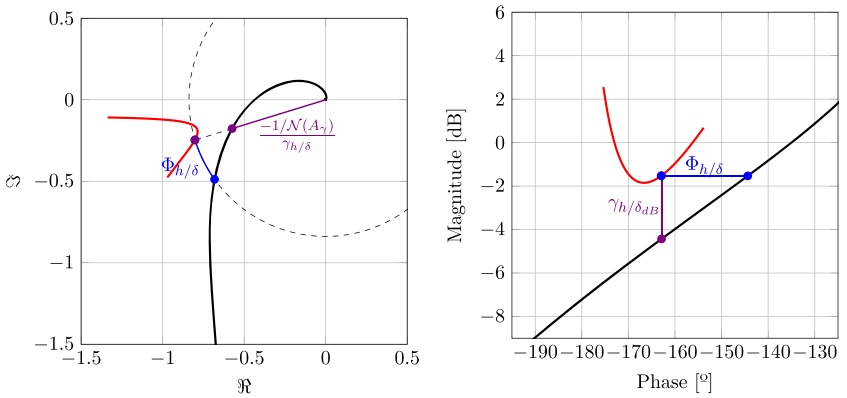

Fig. 6. Graphical representation of the gain and phase margins to the non-linearity ($\gamma_{h/\delta}, \Phi_{h/\delta}$) in Nyquist (left) and Nichols (right) diagrams for the PI controller obtained in Example 1.

Example 1. Consider a system whose transfer function is defined by:

$$G(s) = \frac{1}{(s+1)^4}. \tag{22}$$

The peak-to-peak amplitude of the measurement noise has a magnitude of $e_{n_{p-p}} = 0.03$ and the maximum admissible steady-state error is $e_{ss} = 0.1$.

With the aim of avoiding burst of events introduced by an insufficient hysteresis in the sampler due to the noise, the hysteresis h must be slightly greater than the peak-to-peak amplitude of the noise, thus we choose $h = 0.04$. The upper bound of δ, once h has been chosen, is calculated with the expression of the e_{ss} in RQH loops, $\delta = 2e_{ss} - h$. We choose $\delta = 0.16$, which is the upper bound, in order to keep the quotient h/δ low enough to reduce the number of events and to minimize the effect of the margins $\gamma_{h/\delta}$ and $\Phi_{h/\delta}$ in the controller design.

In order to obtain a proper closed-loop response and enough robustness against limit cycles induced by the sampler, the controller is designed to meet the following constrains:

$$\gamma_{cg} \geq 6\,dB \qquad \Phi_{cp} \geq 45^\circ$$
$$\gamma_{h/\delta} \geq 2\,dB \qquad \Phi_{h/\delta} \geq 15^\circ$$

By applying the proposed tuning procedure we obtain a PI controller with $K_p = 1.05$ and $T_i = 2.6$ whose exact robustness margins are:

$$\gamma_{cg} = 7.22\,dB \qquad \Phi_{cp} = 45^\circ$$
$$\gamma_{h/\delta} = 2.91\,dB \qquad \Phi_{h/\delta} = 18.6^\circ$$

which fulfill the requirements stated above. The robustness margins to the non-linearity can be visualized in Fig. 6, where phase and gain margin to the non-linearity have been represented in Nyquist and Nichols diagrams. Fig. 7 shows the closed-loop response to step changes in the reference and the disturbance inputs. As expected, neither limit cycle oscillations take places nor unnecessary events are generated due to the noise. The amplitude of the control action bumps is $\delta_u = K_p\delta = 0.168$.

In order to show the effect of limiting δ_u on the design, let us consider the actuator to admit a maximum control action variation of $\delta_{u_{\max}} = 0.05$. Taking into account this addi-

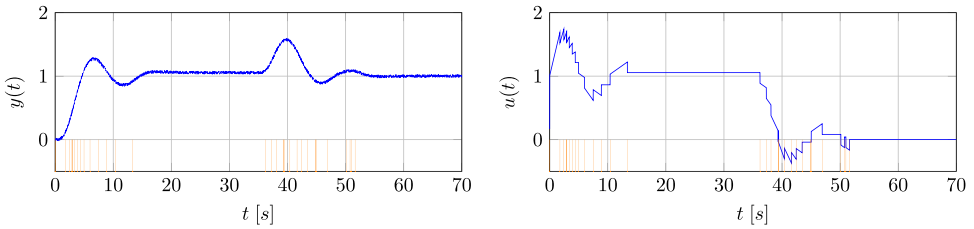

Fig. 7. Time response of the controlled output and control action to unitary step-like changes in reference and disturbance of the example system with the proposed controller and sampler.

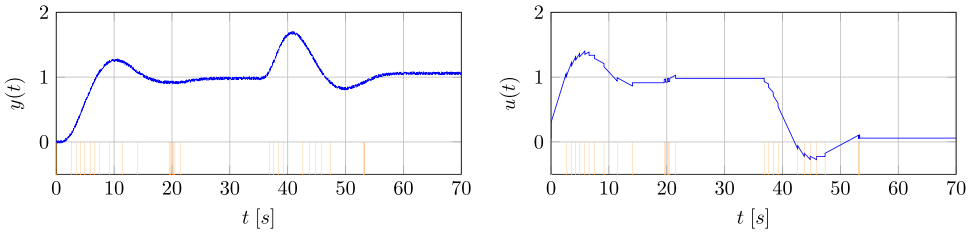

Fig. 8. Time response of the controlled output and control action to unitary step-like changes in reference and disturbance of the example system considering a limitation on the actuator $\delta_u = 0.05$.

tional restriction the new parameters for the controller are $K_p = 0.312$ and $T_i = 1.037$ and the robustness margins:

$$\gamma_{cg} = 9.5126\,dB \qquad \Phi_{cp} = 45^\circ$$
$$\gamma_{h/\delta} = 4.486\,dB \qquad \Phi_{h/\delta} = 20.95^\circ$$

The time response of the controlled system is shown in Fig. 8. As it can be seen, the value of δ_u is limited to 0.05 and consequently a smoother control action is achieved.

In most cases, bigger ratios of h/δ lead to more restrictive robustness constraints for design the controllers. This fact could induce the idea that those PI designed for ratios h/δ bigger than the one to be actually implemented in the system always fulfill all the robustness margins and consequentially the most conservative designs are achieved for the SSOD sampler. The following example shows a case that refutes this assumption.

Example 2. Consider a system whose transfer function is modeled by:

$$G(s) = \frac{e^{-5s}}{(s+1)^3}. \tag{23}$$

For this example consider that the tuning requirements to be met are:

$$\gamma_{cg} \geq 6\,dB \qquad \Phi_{cp} \geq 45^\circ$$
$$\gamma_{h/\delta} \geq 4\,dB \qquad \Phi_{h/\delta} \geq 30^\circ$$

Assume that by applying the procedure to select δ and h taking into account the noise and e_{ss}, the required sampler has a ratio $h/\delta = 1/20$. However, according to the misconception explained before, in order to have a more robust controller, we decide to apply the tuning algorithm considering a sampler with ratio $h/\delta = 1$, i.e. the SSOD sampler.

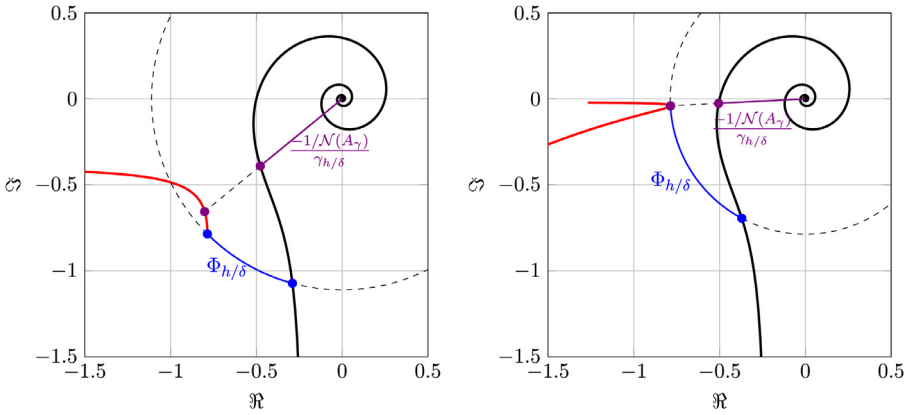

Fig. 9. Gain and phase margins to the non-linearity ($\gamma_{h/\delta}$, $\Phi_{h/\delta}$) obtained in Example 2 for SSOD sampler (left) and sampler with ratio $h/\delta = 1/20$ (right).

The resulting PI has $K_p = 0.518$, $T_i = 5.584$ and classical gain and phase margins $\gamma_{cg} = 6.02\ dB$ and $\Phi_{cp} = 72.1^\circ$. Referring to the robustness against limit cycles, for the SSOD sampler the margins to the non-linearity are $\gamma_{h/\delta} = 4.5072\ dB$ and $\Phi_{h/\delta} = 30^\circ$, fulfilling the requirements. However, the margins for the sampler with ratio $h/\delta = 1/20$ are $\gamma_{h/\delta} = 3.8261\ dB$ and $\Phi_{h/\delta} = 59^\circ$. As it can be noted, the PI designed for SSOD does not fulfill the robustness condition when used with the RQH sampler: in this case $\gamma_{h/\delta}$ is reduced from 4.5072 dB to 3.8261 dB.

A graphical representation of the margins to the non-linearity is presented in Fig. 9 where it can be easily seen the effect of reducing the hysteresis on the margins. In this case, the phase margin to the non-linearity increases as expected because of the folding of the DF traces, however, the gain margin to the non-linearity worsens to the point of not fulfilling the tuning requirements, which is also due to the folding of the DF traces over the real axis.

From the precedent example it can be deduced that the controller needed to fulfill the requirements must be changed if the sampling strategy varies. The following example presents a comparison between the controllers obtained with the proposed method for the specific cases of SSOD and RQH.

Example 3. Let us consider the scenario presented in Example 1, i.e. same process, noise peak-to-peak amplitude and maximum steady-state error. The choice of the RQH sampler will be kept too.

There is a range of the parameter δ for the SSOD sampler to fulfill the noise and error requirements. This range is defined by the same equations than for the RQH but having $h = \delta$, resulting in:

$$e_{n_{p-p}} < \delta < e_{ss}$$

As choosing a value of δ close to $e_{n_{p-p}}$ will result in a high event generation rate, a value $\delta = 0.1$ will be chosen, i.e. at the limit of the admissible maximum steady-state error.

Table 1
Controllers and performance indexes for each controller and sampler under restrictions S_1 and S_2.

		K_p	T_i	$IA\bar{E}_{ref}$	$t_{s,ref}$	$IA\bar{E}_d$	$t_{s,d}$	n_{ev}
S_1	**RQH**	1.01	2.5	4.545	13.899	3.538	17.678	26
	SSOD	0.817	2.57	4.701	17.334	3.795	15.578	34
S_2	**RQH**	0.822	3.081	3.582	5.488	3.285	10.508	16
	SSOD	0.997	5.049	4.895	18.794	4.747	23.498	26

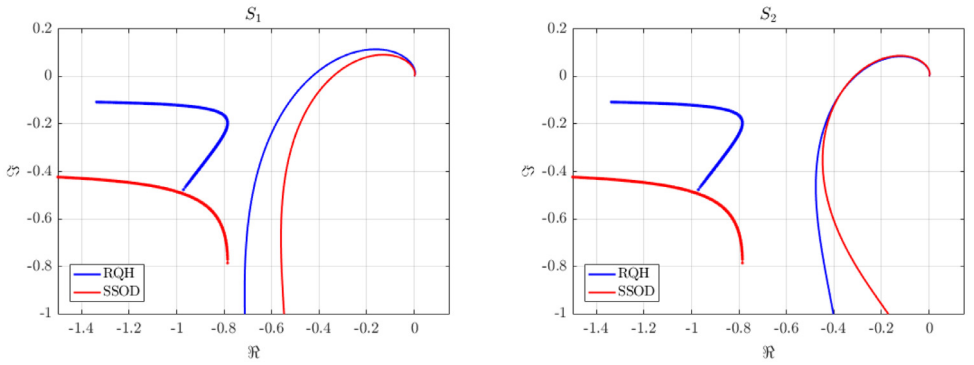

Fig. 10. Nyquist plot of G_{ol} with the obtained controllers and the inverse negative of the DF for both scenarios.

We will consider two sets of robustness requirements to illustrate different situations. These sets denoted by S_1 and S_2 present the following robustness requirements:

$$S_1: \quad \gamma_{cg} \geq 6\,dB \quad \Phi_{cp} \geq 45^\circ \qquad S_2: \quad \gamma_{cg} \geq 6\,dB \quad \Phi_{cp} \geq 45^\circ$$
$$\gamma_{h/\delta} \geq 3\,dB \quad \Phi_{h/\delta} \geq 15^\circ \qquad \gamma_{h/\delta} \geq 3\,dB \quad \Phi_{h/\delta} \geq 45^\circ$$

S_2 presents higher restrictions than S_1 in terms of the phase margin to the non-linearity, therefore, the robustness against limit cycle oscillations will be higher.

Applying the proposed tuning procedure for each set of restrictions and for each sampling strategy four controllers are obtained, whose parameters are gathered in Table 1. The open-loop transfer function for both cases under the specified scenarios can be observed in Fig. 10.

To asses the performance of the controllers several measures will be defined. Firstly, the integral of the absolute sampled error, i.e. at the output of the sampler, as a consequence of a unitary step-like change in the reference ($IA\bar{E}_{ref}$) and disturbance ($IA\bar{E}_d$) inputs. It is defined as:

$$IA\bar{E} = \int_0^\infty |\bar{e}(t)|dt,$$

being $t = 0s$ the point in time where the excitation occurs. In addition, as the classical settling time cannot really be applied due to the appearance of e_{ss}, therefore, the settling time used is defined as the elapsed time from the excitation application to the time at witch the system response enters and remains within the final detection thresholds. Finally, the number of triggered events are also used as a measure.

The temporal responses of the four controllers against step-like changes at the reference and disturbance inputs are presented in Fig. 11, where the RQH case is represented in blue and the SSOD in red. Considering the case presented by the set of conditions S_1, it can be seen

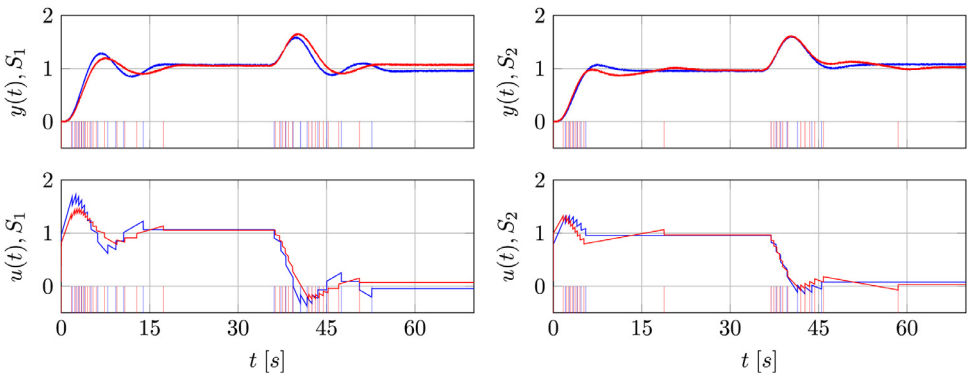

Fig. 11. Temporal response of the measured output of the process with the controllers obtained in Example 3 (blue: RQH and red: SSOD), the events generated and their respective control actions to unitary step changes in the reference (at $t = 0s$) and disturbance (at $t = 35s$) inputs. (For interpretation of the references to colour in this figure legend, the reader is referred to the web version of this article.)

that the temporal responses of both controllers and samplers do not differ significantly. RQH sampling presents bigger changes in the control action produced by the quantification δ used, which leads to a slightly more oscillatory response with a higher overshoot. In Table 1 the performance measures described above is presented, revealing that the usage of RQH sampling entails a reduction on the number of events needed to control the system, and according to the obtained performance indexes, this reduction of events does not degrade the performance of the system.

However, in the set of restrictions S_2, it can be seen a significant improvement of RQH sampling with regard to SSOD. As expected, the number of events generated is lower for RQH, but in addition, the rest of performance indexes are improved. This is due to the slowness of the SSOD controller, resulting from the required robustness against limit cycle oscillations, which produces a slow response that worsens the performance.

In summary, this example shows how by choosing RQH sampling a robust controller against limit cycle oscillations induced by the sampler can be tunned without degrading significantly the overall performance of the system. An opposed situation is found with SSOD sampling, in which to attain similar levels of robustness than in RQH the controller is forced to present a slower response that degrades the system performance. Additionally, the number of events needed for control is lower for RQH than for SSOD regardless of the robustness to attain.

To highlight the importance of the proposed tuning method over other existing tuning rules let us introduce the following example:

Example 4. Consider the process with transfer function:

$$G(s) = \frac{1 - s}{(s + 1)^3}.$$

The peak-to-peak amplitude of the measurement noise has been measured to be of 0.04 units and it is required that the response do not present a steady-state error greater than 0.075. With this requirements a RQH sampler is chosen with $h = 0.05$ to avoid burst of events due to the noise and $\delta = 0.1$ to not surpass the maximum e_{ss} admissible.

Table 2
Obtained controller and performance parameters for each tuning method.

	K_p	T_i	$IA\bar{E}_{ref}$	$t_{s,ref}$	$IA\bar{E}_d$	$t_{s,d}$	n_{ev}
Proposed	0.6646	2.1206	4.8637	14.878	4.1017	13.798	41
AMIGO	0.2473	1.8807	7.4872	18.088	7.7062	22.048	31
One-Third	0.3202	2.8453	8.6168	24.088	8.6736	27.388	31
Ziegler-Nichols	0.9257	6.0792	6.3643	30.268	6.3643	34.768	43

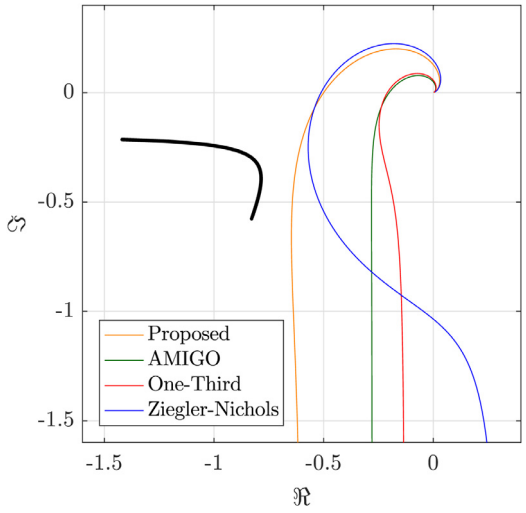

Fig. 12. Inverse negative of the sampler's DF in this example and the $G_{ol}(j\omega)$ of the four studied controllers and process.

A comparative test will be conducted between the performance offered by the proposed tuning method and other well-known methods, namely, AMIGO [35], One-Third [36] and Ziegler-Nichols [37] tuning rules. For our tuning method a controller will be tunned to meet the following constrains:

$$\gamma_{cg} \geq 6\,dB \qquad \Phi_{cp} \geq 45^\circ$$
$$\gamma_{h/\delta} \geq 2\,dB \qquad \Phi_{h/\delta} \geq 15^\circ$$

For the other tuning rules the temporal response of the process has been approximated by a FOPTD model and their parameters have been obtained. The obtained parameters can be seen in Table 2. Needles to say, the controllers tuned with tuning rules other than the proposed in this papers are not supposed to avoid the intersection with the inverse negative of the DF, and therefore, avoid limit cycle oscillations. In this case, all controllers avoid intersection with the DF traces, in deed, the classical tuning rules present higher robustness measures than the proposed method, which can be appreciate in Fig. 12 where the open-loop transfer function of the four controllers and process in the Nyquist diagram is presented as well as the inverse negative of the DF of the sampler under study.

The temporal response of the controlled output can be found in Fig. 13 as well as the generated events and the control action. In order of appearance: the proposed controller (orange), AMIGO (green), One-Third (red) and Ziegler-Nichols (blue) tuning rules. As it can be

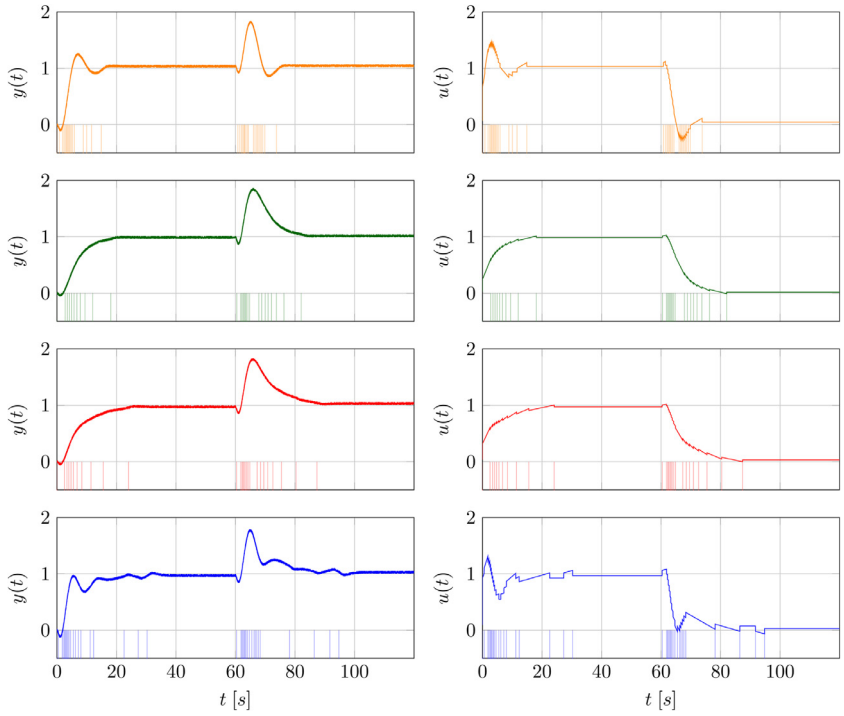

Fig. 13. Temporal response of the measured output of the process with different controllers, the events generated and their respective control action to unitary step changes in the reference (at $t = 0s$) and disturbance (at $t = 60s$) inputs. (Orange: proposed controller. Green: AMIGO. Red:One-Third. Blue: Ziegler-Nichols).

seen, all the controllers present enough robustness to avoid limit cycle oscillations. AMIGO and One-Third tuning rules present controllers with a slow temporal response compared to the other rules, however, this is a normal behavior since they also present the highest robustness. The other controllers present a faster response, nevertheless, Ziegler-Nichols struggles to stabilize more than the proposed method.

The measures presented in Example 3 have been used to evaluate the performance of the controllers under study, and have been summarized in Table 2. As it can be seen, the proposed tuning rule presents the fastest results, being its integral errors and settling times, both under reference and disturbance changes, the ones with lower values. However, it presents a greater generation event rate, as Ziegler-Nichols, when compared with AMIGO and One-Third tuning rules. This is due to the overdamped temporal response of these last two methods, which matches with its increased robustness and slowness in the response.

4. Design validation

The gain and phase margins to the non-linearity used in the tuning procedure were obtained using the DF technique, which assumes that the filtering capabilities of the linear part of the system are good enough to neglect the high order harmonics effect at the input of the non-linearity. If this assumption is not fulfilled, the DF viability for predicting limit cycle can

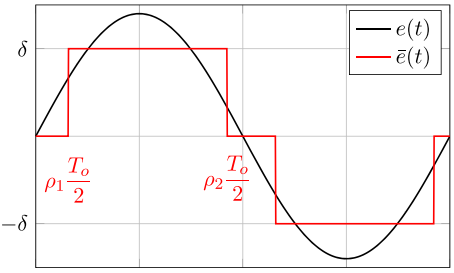

Fig. 14. Sinusoidal signal and its sampled output with a sampler with a given ratio h/δ.

conduct to misleading results. In this section, we analyze the effect of high order harmonics on the proposed margins by studying the variation of the critical points to which each margin is measured. Therefore, the results presented in this section can be used to validate the design procedure presented before or any other tuning method that uses $\gamma_{h/\delta}$ and $\Phi_{h/\delta}$ to check the robustness against limit cycles induced by the RQH sampler.

Consider the input to the non-linearity to be a sine wave with period T_o and amplitude A, which is considered high enough to produce single-leveled symmetric oscillations ($m = 1$) on the sampled signal $\bar{e}(t)$ as it is shown in Fig. 14. The switches on the sampled signal $\bar{e}(t)$ are produced at the time fractions ρ_1 and ρ_2. In those switching points the value of the error signal $e(t)$ is:

$$e\left(\rho_p \frac{T_o}{2}\right) = \begin{cases} \delta\left(\frac{1}{2} + \frac{h}{2\delta}\right) & \text{for } p = 1 \\ \delta\left(\frac{1}{2} - \frac{h}{2\delta}\right) & \text{for } p = 2 \end{cases} \tag{24}$$

As a sinusoidal signal has been supposed at the input of the non-linearity, the value of the time fractions ρ_1 and ρ_2 can be obtained:

$$\begin{aligned} \rho_1 &= \frac{1}{\pi} \arcsin\left(\frac{\delta}{A}\left(\frac{1}{2} + \frac{h}{2\delta}\right)\right) \\ \rho_2 &= 1 - \frac{1}{\pi} \arcsin\left(\frac{\delta}{A}\left(\frac{1}{2} - \frac{h}{2\delta}\right)\right) \end{aligned} \tag{25}$$

Expressing the sampled signal $\bar{e}(t)$ as a Fourier series, and operating with the obtained expression of this signal through the loop, considering $y_r(t) = 0$, and thus, $e(t) = -y(t)$, it can be obtained the resulting expression of $e(t)$, in which, evaluating at $t = \rho_1 \frac{T_o}{2}$ and $t = \rho_2 \frac{T_o}{2}$:

$$e\left(\rho_1 \frac{T_o}{2}\right) = -\frac{4\delta}{\pi} \sum_{n_{odd}}^{\infty} \frac{1}{n} \left[\Re\{G_{ol}(jn\omega_o)\} \frac{1}{2} \sin(n\pi(\rho_2 - \rho_1)) + \Im\{G_{ol}(jn\omega_o)\} \sin^2\left(\frac{n\pi}{2}(\rho_2 - \rho_1)\right) \right]$$

$$e\left(\rho_2 \frac{T_o}{2}\right) = -\frac{4\delta}{\pi} \sum_{n_{odd}}^{\infty} \frac{1}{n} \left[\Re\{G_{ol}(jn\omega_o)\} \frac{1}{2} \sin(n\pi(\rho_2 - \rho_1)) - \Im\{G_{ol}(jn\omega_o)\} \sin^2\left(\frac{n\pi}{2}(\rho_2 - \rho_1)\right) \right]$$

substituting these values of $e(t)$ in the switching points presented in Eq. (24), this equation can be expressed otherwise as:

$$\Re\{G_{ol}(j\omega_o)\} = -\frac{\frac{\pi}{4} + \sum_{n=3,5,\dots}^{\infty} \frac{1}{n}\Re\{G_{ol}(jn\omega_o)\}\sin(n\pi(\rho_2-\rho_1))}{\sin(\pi(\rho_2-\rho_1))}$$
$$\Im\{G_{ol}(j\omega_o)\} = -\frac{\frac{\pi h}{8\delta} + \sum_{n=3,5,\dots}^{\infty} \frac{1}{n}\Im\{G_{ol}(jn\omega_o)\}\sin^2\left(\frac{n\pi}{2}(\rho_2-\rho_1)\right)}{\sin^2\left(\frac{\pi}{2}(\rho_2-\rho_1)\right)}$$

Replacing the expressions of ρ_1 and ρ_2 which were obtained in Eq. (25), the previous expressions can be rewritten as:

$$\begin{aligned}\Re\{G_{ol}(j\omega_o)\} &= -\frac{\frac{\pi}{4} + \sum_{n=3,5,\dots}^{\infty} \frac{1}{n}\Re\{G_{ol}(jn\omega_o)\}\sin(n\theta)}{\sin(\theta)} \\ \Im\{G_{ol}(j\omega_o)\} &= -\frac{\frac{\pi h}{4\delta} + \sum_{n=3,5,\dots}^{\infty} \frac{1}{n}\Im\{G_{ol}(jn\omega_o)\}(1+\cos(n\theta))}{1+\cos(\theta)}\end{aligned} \tag{26}$$

where:

$$\theta = \arcsin\left(\frac{\delta}{2A}\left[\left(1-\frac{h}{\delta}\right)\sqrt{1-\left[\frac{\delta}{2A}\left(1+\frac{h}{\delta}\right)\right]^2} + \left(1+\frac{h}{\delta}\right)\sqrt{1-\left[\frac{\delta}{2A}\left(1-\frac{h}{\delta}\right)\right]^2}\right]\right)$$

which depends on the non-linearity characteristics.

Eq. (26) describe the real and imaginary parts of $G_{ol}(j\omega_o)$ when the system presents oscillation of frequency ω_o. As it can be seen, these expressions depend on the high order harmonics of the oscillation frequency: $n\omega_o, n = 3, 5, \dots,$ which are neglected in the DF approach. Therefore, these equations can be used to validate the controllers obtained by the tuning method proposed in Section 3. To do that, more accurate estimations of the points with respect to which the margins $\gamma_{h/\delta}$ and $\Phi_{h/\delta}$ are measured can be obtained by using equations in (26) with a reasonable number of harmonics and the values of $G_{ol}(jn\omega_o)$, $n = 3, 5, \dots$ approximated as:

$$G_{ol}(jn\omega_o) = G_{ol}(jn\omega_\gamma)\gamma_{h/\delta}; \quad n = 3, 5, \dots \tag{27}$$

for evaluating the gain margin accuracy, and:

$$G_{ol}(jn\omega_o) = G_{ol}(j\omega_\Phi)\cdot 1\angle -\Phi_{h/\delta}; \quad n = 3, 5, \dots \tag{28}$$

for evaluating the phase margin. In fact, Eqs. (27) and (28) provide the values G_{ol} in the higher order harmonics of frequencies where the oscillations will take place if the gain or phase lag of G_{ol} increase on $\gamma_{h/\delta}$ or $\Phi_{h/\delta,}$ respectively.

Hence, to validate the gain and phase margin to the non-linearity obtained, and therefore, the controller that has been tuned, the point obtained using Eqs. (26) and (27), which will be denoted by $G_{ol,\gamma}(j\omega_o)$, has to be compared to the point $-1/\mathcal{N}(A_\gamma)$. Similarly, the point obtained with Eqs. (26) and (28), which we will be referred to as $G_{ol,\Phi}(j\omega_o)$, has to be compared to the point $-1/\mathcal{N}(A_\Phi)$.

To show the variation of these critical points with respect to those where the gain and phase margin to the non-linearity are measured and how this variation is used to validate the proposed controllers, let us introduce the following example.

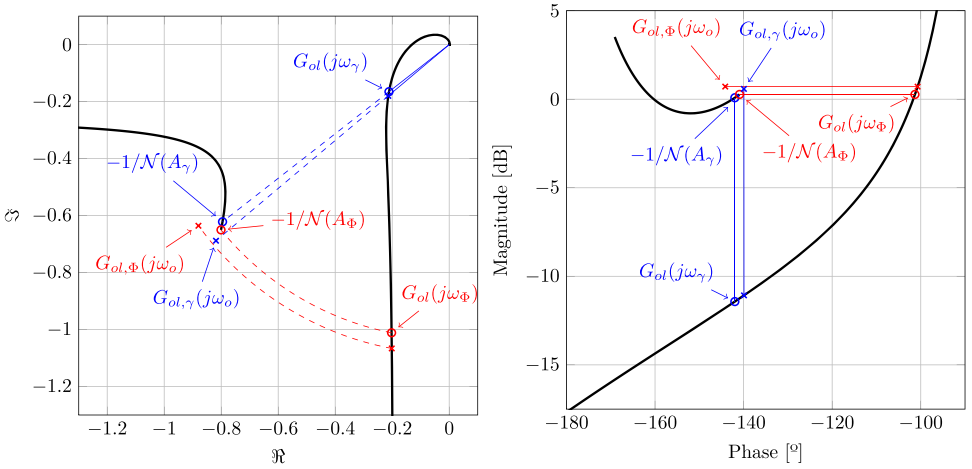

Fig. 15. Harmonic analysis of the validity of the proposed margins for $G_{ol}(s)$ and the sampler with ratio $h/\delta = 2/3$.

Example 5. Consider a system whose transfer function is defined by:

$$G(s) = \frac{1}{(s+1)^4}.$$

A PI controller has been tuned applying AMIGO method [35] by approximating this system by a FOPTD model, obtaining $K_p = 0.301$ and $T_i = 2.4268$. Consider in this case that the system is placed in a loop which contains a sampler with ratio $h/\delta = 2/3$. The robustness margins to the non-linearity have been measured and result in $\gamma_{h/\delta} = 11.51$ dB and $\Phi_{h/\delta} = 39.61°$. The gain margin has been obtained at a frequency $\omega_\gamma = 0.4703$ rad/s and with a ratio $\delta/A = 0.834$, while the phase margin has been obtained at a frequency $\omega_\Phi = 0.1218$ rad/s and with a ratio $\delta/A = 0.833$.

The points where these measures have been obtained can be seen graphically in Fig. 15, where it has been represented the negative inverse of the DF and $G_{ol}(j\omega)$ in solid black line and the measured robustness margins with a circle marker, in blue for the gain margin and in red for the phase margin, in the Nyquist and Nichols diagrams.

Then, to test the validity of the margins, Eq. (26) have been used considering the following 3 harmonics: $n = 3$, 5 and 7. In those equations, the open-loop transfer function to test is the one presented in Eq. (27) to test the gain margin and (28) to test the phase margin.

As a result, the new location of the critical points is obtained. These new points have been represented with a cross of its respective color in Fig. 15, and the respective new robustness margins have been measured to these points. In this case, the variation between $-1/\mathcal{N}(A_\gamma)$ and $G_{ol,\gamma}(j\omega_o)$ and between $-1/\mathcal{N}(A_\Phi)$ and $G_{ol,\Phi}(j\omega_o)$ is not very important. Thus, as the variation between the robustness margins is very slight, being both obtained margins more restrictive than the corrected margins considering the high order harmonic contribution, the obtained controller can operate safely in this loop.

Nevertheless, the corrected margins are not always beneficial in terms of robustness. For example, consider now that the sampler used above is replaced by another sampler with ratio $h/\delta = 1/6$. As in the precedent case, the robustness measures to the non-linearity have been obtained at the critical frequencies and δ/A ratios. Using Eqs. (26)–(28) as it has been

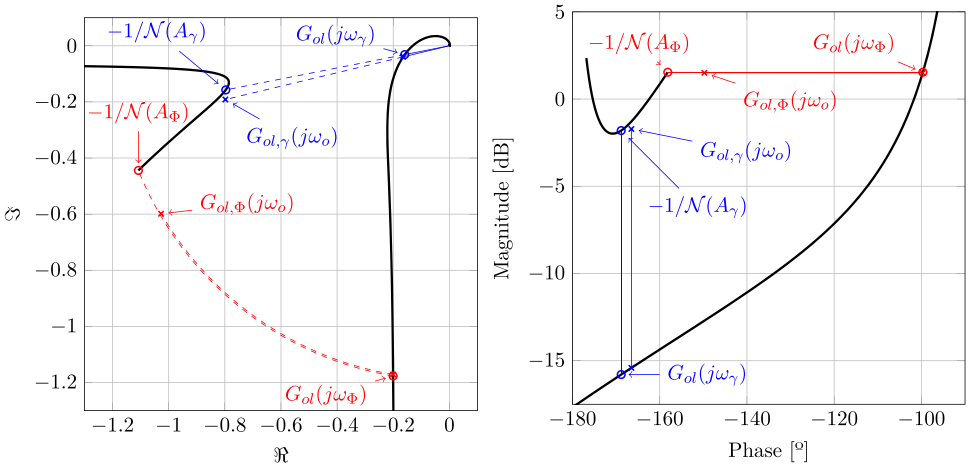

Fig. 16. Harmonic analysis of the validity of the proposed margins for a given system and sampler.

explained before, the new location of the critical points has been obtained. In Fig. 16 it has been represented the negative inverse of the DF traces, the transfer function and the critical points obtained with the DF and with the harmonic analysis calculus. Here it can be seen that the variation of the critical points implies a reduction in the effective margins, being this reduction more visible in the case of the phase margin.

In this case, the variation in the margins is not significant enough to induce limit cycle oscillations in the temporal response, in fact, considering the new recalculated margins, the controller still provides a considerable degree of robustness to the system. However, this proves that the influence of high order harmonics is not always beneficial in terms of robustness and that the validation of the controller design should be carried out, specially when systems with low filtering capabilities are involved, because the DF approach cannot be applicable with a high reliability.

In general lines, the proposed margins give an accurate order of magnitude of the proximity to the oscillations due to the effect of the non-linearity. As it has been seen in the precedent example, the effect of the high order harmonics takes an important role in the accuracy of the robustness margins to the non-linearity, being the variation of the critical points beneficial or detrimental depending on the case.

In particular, in those cases where $\Phi_{h/\delta}$ is obtained for relative low values of ω_Φ, the variation of the critical point of the phase margin produced by the harmonic analysis is more remarkable, resulting in decreasing the effective phase margin to the non-linearity. In those cases, despite the variation on the phase margin, the corrected phase margin measure still provides enough robustness.

5. Conclusions

In this paper a tuning procedure for PI controllers within a loop with a RQH sampling strategy has been provided. Prior to the controller tuning the parameters that define the RQH

sampler must be chosen. Guidelines to select the proper parameters for a system from specifications have been provided.

The tuning procedure consists of 3 steps in which both, the classical robustness margins and the robustness margins to the limit cycles produced by the sampler proposed in this paper, have been taken into account. By considering both, not only the limit cycle oscillations induced by the sampler are avoided, but also a proper closed-loop temporal response is assured.

Several simulation examples where the proposed tuning method is applied are shown. Those examples illustrate the usefulness of the method and how a loss in robustness can be suffered when the method is not properly used.

Finally, the validation of the controller design has been tested by considering the effect on the robustness measures of higher order harmonics. In the cases where the DF technique can be used, it has been confirmed that the proposed margins to predict the appearance of oscillations are accurate and this validation can be skipped. Nevertheless, in those cases where systems with low filtering capabilities are involved the validation of the controller designed is recommendable due to the high order harmonic influence on the robustness.

6. Future works

In this section two work lines for future researches related with the tuning of controllers with RQH sampling strategy are presented, which, in the opinion of the authors, could significantly improve the applicability and performance of this kind of control system:

1. The tuning procedure proposed in this paper is based on shaping the open-loop transfer function to obtain both the desired robustness margins and good closed-loop performance for a kind of event-based control loop with a continuous PI controller and RQH sampler. As it has been shown, this goal can be successfully achieved with a conventional PI controller by selecting the proper parameters K_p and T_i. Other controller structures, such as PID, could provide more flexibility on configuring G_{ol}, and consequently, a better trade-off between robustness and response speed can be attained using that control structure. In this sense, the use of fractional order PID controllers seems specially interesting since they are a generalization of the conventional PID with more degrees of freedom in their frequency response due to the fractional-order differential and integral operators [38]. Fractional order PID is a consolidated field of research with a growing acceptance by the practitioner [39–42]. Because the suitability of the describing function technique in the context of fractional order systems has been previously shown in [29,43,44], the extension of the results presented in this paper for fractional order control systems could lead to promising results in the field of EBC.
2. It is known that the validity of the describing function technique depends on the filtering properties of the linear part of the control loop. Consequently, the application of this technique for low order systems, such as first order plus time delay (FOPTD), is questionable. Because FOPTD models are commonly used to approximate the behavior of many actual industrial processes, it is worth considering more proper approaches for tuning RQH based controllers for this kind of systems. In [34] a procedure for tuning PI and PID controllers with SSOD sampling for processes with a FOPTD model was proposed by the authors. The approach is based on a new robustness measure to avoid limit cycle oscillations induced by the SSOD sampler, called the Tsypkin margin, which overcomes the limitations of DF approaches. The extension to RQH sampling of the results presented by the authors in

[45] could be of interest for tuning RQH based controllers for processes whose dynamic is modeled by low order transfer functions.

Declaration of Competing Interest

The authors declare that they have no known competing financial interests or personal relationships that could have appeared to influence the work reported in this paper.

Acknowledgments

This work has been supported by MICINN project number TEC2015-69155-R from the Spanish government, research project 18I411-Uji-b2018-39 from Universitat Jaume I and by CEICE grant number ACIF/2018/244.

Appendix A. Validity of IE index

In the nature of the $EG - C(s)$ control loops is to have a static position error bounded by the switching thresholds of the chosen sampling strategy. Thus, the choice of IE index for selecting a controller can be questioned because it will tend to infinite. For this reason, a modification of this index has been considered using the sampled error signal $\bar{e}(t)$ instead of the error signal $e(t)$, because it tends to 0 in steady state, producing the sampled integral error index $I\bar{E}$, defined as:

$$I\bar{E} = \int_0^\infty \bar{e}(t)dt.$$

The control action for this kind of non-linear systems is:

$$u(t) = K_p\bar{e}(t) + K_i\int_0^t \bar{e}(\tau)d\tau - K_\mathrm{d}\frac{dy}{dt},$$

which for a PI controller:

$$u(t) = K_p\bar{e}(t) + K_i\int_0^t \bar{e}(\tau)d\tau.$$

Considering a step change at the disturbance input, in steady-state (assuming stability):

$$u(\infty) = K_p\bar{e}(\infty) + K_i\int_0^\infty \bar{e}(t)dt,$$

as $\bar{e}(\infty) = 0$ and taking into account the expression of $I\bar{E}$:

$$u(\infty) = K_i\int_0^\infty \bar{e}(t)dt = K_iI\bar{E}$$

From the schema block in Fig. 1:

$$(u(\infty) + p(\infty))G(0) = y(\infty) = -e(\infty),$$

where $e(\infty)$ is bounded by the steady state error e_{ss}, and, as a unitary step load disturbance is assumed $p(\infty) = 1$:

$$(u(\infty) + 1)G(0) \leq e_{ss},$$

substituting with the expression of $u(\infty)$:

$$\left(K_i I\bar{E} + 1\right)G(0) \leq e_{ss},$$

taking into account that the IE caused by a load disturbance is $-1/K_i$:

$$I\bar{E} \leq \frac{e_{ss}}{K_i G(0)} + IE,$$

from which the difference between both indexes can be found:

$$I\bar{E} - IE \leq \frac{e_{ss}}{K_i G(0)}.$$

In this last expression it appears the relation between $I\bar{E}$ and IE indexes. Here it can be seen that the effect of maximizing K_i minimizes the IE index, and makes the difference $I\bar{E} - IE$ minimum. In addition, as the system is assumed stable, the static error is bounded between:

$$e_{ss} \in \left(-\frac{\delta + h}{2}, \frac{\delta + h}{2}\right)$$

thus, choosing proper values of δ and h, and maximizing K_i, the contribution of e_{ss}, i.e. the effect of the sampling, can be small enough to consider $IE \approx I\bar{E}$, and thus, we can consider the IE an appropriate selection index for PI tuning.

Appendix B. Flowchart of the tuning procedure

The proposed tuning procedure can be deployed by following the steps in this flowchart:

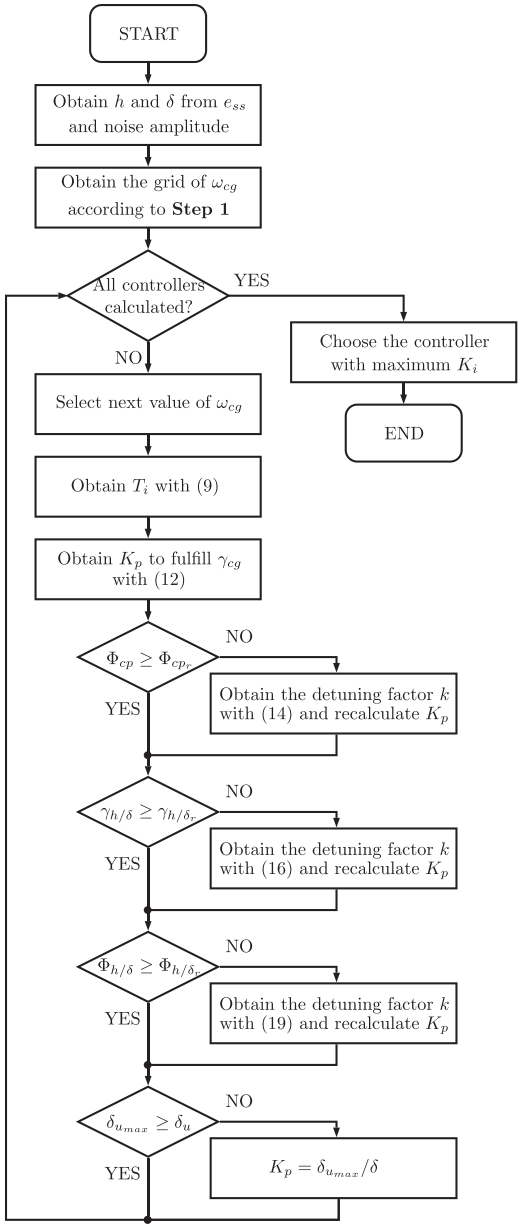

Fig. B1. Flowchart that summarizes the tuning procedure.

References

[1] J. Lunze, Event-based control: introduction and survey, in: M. Miskowicz (Ed.), Event-Based Control and Signal Processing, Boca Raton: CRC Press, 2015, pp. 3–20, doi:10.1201/b19013-3.

[2] M. Dotoli, A. Fay, M. Miśkowicz, C. Seatzu, An overview of current technologies and emerging trends in factory automation, Int. J. Prod. Res. 57 (15–16) (2019) 5047–5067, doi:10.1080/00207543.2018.1510558.

[3] E. Aranda-Escolástico, M. Guinaldo, R. Heradio, J. Chacón, H. Vargas, J. Sánchez, S. Dormido, Event-based control: a bibliometric analysis of twenty years of research, IEEE Access 8 (March) (2020) 47188–47208, doi:10.1109/ACCESS.2020.2978174.
[4] K.J. Åström, T. Hägglund, K.J. Astrom, Advanced PID Control, 461, ISA-The Instrumentation, Systems, and Automation Society Research Triangle, 2006.
[5] T. Samad, A survey on industry impact and challenges thereof, IEEE Control Syst. 37 (1) (2017) 17–18, doi:10.1109/MCS.2016.2621438.
[6] A. Maxim, D. Copot, C. Copot, C.M. Ionescu, The 5w's for control as part of industry 4.0: why, what, where, who, and when-A PID and MPC control perspective, Inventions 4 (1) (2019), doi:10.3390/inventions4010010.
[7] T.C. Hsia, Analytic design of adaptive sampling control law in sampled-Data systems, IEEE Trans. Autom. Control 19 (1) (1974) 39–42, doi:10.1109/TAC.1974.1100455.
[8] S. Dormido, J. Sánchez, E. Kofman, Muestreo, control y comunicación basados en eventos, Revista Iberoamericana de Automática e Informática Industrial RIAI 5 (1) (2008) 5–26.
[9] J. Ploennigs, V. Vasyutynskyy, K. Kabitzsch, Comparative study of energy-efficient sampling approaches for wireless control networks, IEEE Trans. Ind. Inf. 6 (3) (2010) 416–424.
[10] K.E. rz, A Simple Event-based PID Controller, in: Proceedings of the 14th World Congress of IFAC, Beijing, 1999, pp. 423–428.
[11] S. Durand, N. Marchand, An event-based PID controller with low computational cost, in: L. Fesquet, B. Torrésani (Eds.), Proceedings of the 8th International Conference on Sampling Theory and Applications (SampTA'09), 2009. http://hal.archives-ouvertes.fr/hal-00393031.
[12] S. Durand, N. Marchand, Further results on event-based PID controller, in: Proceedings of the European Control Conference, Budapest, Hongrie, 2009, pp. 1979–1984. http://hal.archives-ouvertes.fr/hal-00368535.
[13] V. Vasyutynskyy, K. Kabitzsch, A comparative study of PID control algorithms adapted to send-on-delta sampling, in: Proceedings of the IEEE International Symposium on Industrial Electronics (ISIE), 2010, pp. 3373–3379, doi:10.1109/ISIE.2010.5637997.
[14] V. Vasyutynskyy, K. Kabitzsch, Time constraints in PID controls with send-on-delta, in: G. Juanole, S.H. Hong (Eds.), Proceedings of the Fieldbuses and Networks in Industrial and Embedded Systems, volume 8, 2009.
[15] C.I. Muresan, I.R. Birs, E.H. Dulf, Event-based implementation of fractional order IMC controllers for simple FOPDT processes, Mathematics 8 (8) (2020) 1378, doi:10.3390/math8081378.
[16] I. Birs, C.I. Muresan, R. Both, I. Nascu, A real life implementation of fractional order event based PI control, in: Proceedings of the IEEE International Conference on Automation, Quality and Testing, Robotics (AQTR), 2020, pp. 1–6, doi:10.1109/AQTR49680.2020.9129933.
[17] I. Birs, I. Nascu, C. Ionescu, C. Muresan, Event-based fractional order control, J. Adv. Res. 25 (2020) 191–203, doi:10.1016/j.jare.2020.06.024. Recent Advances in the Fractional-Order Circuits and Systems: Theory, Design and Applications
[18] I. Birs, C. Muresan, C. Ionescu, An event based implementation of a fractional order controller on a non-Newtonian transiting robot, Proceedings of the European Control Conference ECC 2020(2020c) 1436–1441. 10.23919/ecc51009.2020.9143776.
[19] M. Beschi, S. Dormido, J. Sánchez, A. Visioli, Characterization of symmetric send-on-delta PI controllers, J. Process Control 22 (10) (2012) 1930–1945.
[20] M. Beschi, S. Dormido, J. Sánchez, A. Visioli, Tuning of symmetric send-on-delta proportional-integral controllers, IET Control Theory Appl. 8 (4) (2014) 248–259, doi:10.1049/iet-cta.2013.0048.
[21] J. Snchez, M. Guinaldo, A. Visioli, S. Dormido, Identification of process transfer function parameters in event-based PI control loops, ISA Trans. 75 (2018) 157–171, doi:10.1016/j.isatra.2018.01.033.
[22] A. Pawlowski, M. Beschi, J.L. Guzmn, A. Visioli, M. Berenguel, S. Dormido, Application of SSOD-PI and PI-SSOD event-based controllers to greenhouse climatic control, ISA Trans. 65 (2016) 525–536, doi:10.1016/j.isatra.2016.08.008. http://www.sciencedirect.com/science/article/pii/S0019057816301707
[23] J.A. Romero, R. Sanchis, I. Peñarrocha, A simple rule for tuning event-based PID controllers with symmetric send-on-delta sampling strategy, in: Proceedings of the 2014 IEEE Emerging Technology and Factory Automation (ETFA), 2014, pp. 1–8, doi:10.1109/ETFA.2014.7005070.
[24] J.A. Romero Pérez, R. Sanchis Llopis, A new method for tuning PI controllers with symmetric send-on-delta sampling strategy, ISA Trans. 64 (2016) 161–173.
[25] A. Ruiz, M. Beschi, A. Visioli, S. Dormido, J.E. Jimnez, A unified event-based control approach for FOPTD and IPTD processes based on the filtered smith predictor, J. Frankl. Inst. 354 (2) (2017) 1239–1264, doi:10.1016/j.jfranklin.2016.11.017.
[26] N.M. Krylov, N.N. Bogoliubov, Introduction to Non-Linear Mechanics, Princeton University Press, 1949.

[27] J.C. West, J.L. Douce, R.K. Livesley, The dual-input describing function and its use in the analysis of non-linear feedback systems, Proc. IEE-Part B Radio Electron. Eng. 103 (10) (1956) 463–473.
[28] E.I. Jury, Sampled-data Control Systems, John Wiley & Sons, Inc., New York, 1958.
[29] J. Tenreiro Machado, Fractional order describing functions, Signal Process. 107 (2015) 389–394, doi:10.1016/j.sigpro.2014.05.012. Special Issue on ad hoc microphone arrays and wireless acoustic sensor networks Special Issue on Fractional Signal Processing and Applications
[30] A. Gelb, W.E. Van der Velde, Multiple-Input Describing Functions and Non-linear System Design, McGraw-Hill, 1968.
[31] A. Nassirharand, Computer-aided Nonlinear Control System Design: Using Describing Function Models, Springer London, 2012.
[32] J.A. Romero Pérez, R. Sanchis Llopis, Tuning and robustness analysis of event-based PID controllers under different event-generation strategies, Int. J. Control (2017) 1–21.
[33] O. Miguel-Escrig, J.-A. Romero-Pérez, Regular quantisation with hysteresis: a new sampling strategy for event-based PID control systems, IET Control Theory Appl. (2020).
[34] O. Miguel-Escrig, J.-A. Romero-Pérez, R. Sanchis-Llopis, Tuning PID controllers with symmetric send-on-delta sampling strategy, J. Frankl. Inst. 357 (2) (2020) 832–862.
[35] K.J. Åström, T. Hägglund, Revisiting the ziegler-Nichols step response method for PID control, J. Process Control 14 (6) (2004) 635–650.
[36] T. Hägglund, The one-third rule for PI controller tuning, Computers & Chemical Engineering 127 (2019) 25–30.
[37] J.G. Ziegler, N.B. Nichols, Optimum settings for automatic controllers, trans. ASME 64 (11) (1942).
[38] C.A. Monje, Y. Chen, B.M. Vinagre, D. Xue, V. Feliu-Batlle, Fractional-order systems and controls, Advances in Industrial Control, 1, Springer-Verlag London, 2010, doi:10.1007/978-1-84996-335-0.
[39] K. Bingi, R. Ibrahim, M.N. Karsiti, S.M. Hassan, V.R. Harindran, Fractional-order Systems and PID Controllers, Studies in Systems, Decision and Control, 1, Springer International Publishing, 2020, doi:10.1007/978-3-030-33934-0.
[40] B. Jakovljevi, P. Lino, G. Maione, Control of double-loop permanent magnet synchronous motor drives by optimized fractional and distributed-order PID controllers, Eur. J. Control (2020), doi:10.1016/j.ejcon.2020.06.005.
[41] M. Pirasteh-Moghadam, M.G. Saryazdi, E. Loghman, E. Ali Kamali, F. Bakhtiari-Nejad, Development of neural fractional order PID controller with emulator, ISA Trans. 106 (2020) 293–302, doi:10.1016/j.isatra.2020.06.014.
[42] B. Liang, S. Zheng, C.K. Ahn, F. Liu, Adaptive fuzzy control for fractional-order interconnected systems with unknown control directions, IEEE Trans. Fuzzy Syst. (2020) 1, doi:10.1109/TFUZZ.2020.3031694.
[43] Y. Luo, Y. Chen, Y. Pi, Fractional order ultra low-speed position servo: improved performance via describing function analysis, ISA Trans. 50 (1) (2011) 53–60, doi:10.1016/j.isatra.2010.09.003.
[44] D. Atherton, N. Tan, C. Yeroglu, G. Kavuran, A. Yce, Limit cycles in nonlinear systems with fractional order plants, Machines 2 (3) (2014) 176–201, doi:10.3390/machines2030176.
[45] O. Miguel-Escrig, J.-A. Romero-Pérez, R. Sanchis-Llopis, Tuning PID controllers with symmetric send-on-delta sampling strategy, J. Frankl. Inst. 357 (2) (2020) 832–862, doi:10.1016/j.jfranklin.2019.10.008.